

ANFIS Based Control of a Grid Connected Hybrid Renewable Energies for Smart Grid Application

P.Sakthikumaresan¹ C.P.Kandasamy²

¹P.G. Scholar ²Assistant Professor

¹Department of Power Systems Engineering ²Department of Electrical & Electronics Engineering
^{1,2}V.S.B Engineering College, Karur, India - 639111

Abstract— In this paper describes and performance an adaptive neuro-fuzzy inference system (ANFIS)-based energy management system (EMS) of a grid-connected hybrid system for smart grid application. As a part of hybrid system consists of wind turbine (WT) and photovoltaic (PV) solar panels as a primary energy sources. Then rectified wind output and solar panel output which combined given to SEPIC converters in order to connect them to a central DC grid. Additionally, it connects the hybrid system to the single-phase inverter and smart grid. This smart grid consists of new bidirectional intelligent semiconductor transformer (BIST), high frequency ac-dc rectifier and low voltage dc-dc converter hybrid switching dc-ac converter.

Key words: ANFIS, SEPIC converter, bidirectional dc/ac converter, Bidirectional Intelligent Semiconductor Transformer (BIST)

I. INTRODUCTION

Currently, renewable energy sources play a major role in electrical energy generation [3],[5]. Power systems are undergoing considerable changes as generation moves from large-centralized conventional power plants to small-decentralized renewable power plants [6]. In reality, the use in these small power plants of hybrid renewable energy systems(HRES), mainly based on renewable sources presents some advantages over larger power plants, such as non-polluted, quality of power, reliable operation, low cost, direct generation, and expandability[6].

A characteristic HRES arrangement integrates several renewable energy sources, such as wind turbine (WT) and photovoltaic (PV) panels. The renewable sources are used as primary energy sources.

Whenever there is wind or solar radiation. On the other hand, because the sun irradiance and the wind speed are uncontrollable parameters. Conventionally, this function is performed by an ANFIS control with PWM technique. These are considered to be a supportive solution to balance the generation and demand [3]-[4]. All renewable sources (rectified ac and solar dc) and are connected together to a central dc bus by means of dc to dc converters. These converters are designed to deliver energy from the energy sources, ensuring stable, sustainable and reliable operation [8].

Intelligent control techniques such as artificial neural networks, fuzzy logic or neuro-fuzzy are more capable and forceful than traditional techniques, since they do not require an exact model of the system and improve the dynamic behavior of the system. Along with the adaptive neuro-fuzzy inference system (ANFIS) is faster in convergence when compared to the other neuro-fuzzy models.

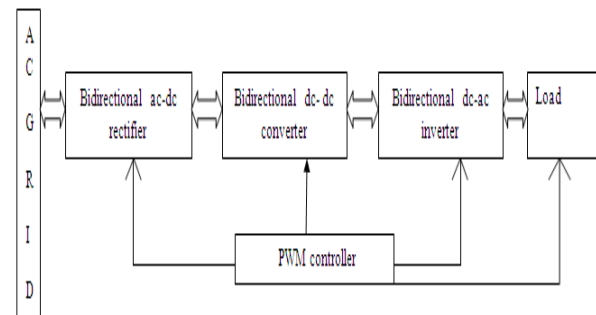


Fig. 1: Configuration of BIST connected to smart grid.

Conventional transformer serene of coil and iron core can change only the magnitude of the ac voltage and the quality of supplying power is totally dependent on that of the input power. Hence, it cannot be appropriate for the smart grid, in which the magnitude and frequency of the operation voltage are different and high-quality power is required [10]. Intelligent semiconductor transformer or solid-state transformer was planned by EPRI to replace the usual transformer in railway systems and substations, in which light weight is mandatorily required. Recently, EPRI has reported 100 KVA single-phase semiconductor transformers named intelligent universal transformer for distribution automation [9].

On the other hand, since the power flow in these transformers is unidirectional, it is not properly applicable for the dc distribution and micro grid [9]-[10]. One can find some studies on the semiconductor transformer topologies with bidirectional power flow capability [7]. The topology [11] in can compensate sag/swell voltage; however, it employs heavy and bulky line-frequency transformer for isolation. The semi-conductor transformer in has not only the bidirectional power flow functions but also voltage sag compensation where high-frequency dc/dc power conversion is employed [12]. The circuit configuration, however, shows too many active switching device counts, at least 18 IGBTs for implementing single-phase module. In three-stage structure comprised of ac/dc converter, dual-active-bridge dc/dc converter, and inverter. This paper proposes a new bidirectional intelligent semiconductor transformer (BIST) for the smart distribution system and micro grid.

The BIST consists of high-voltage part and low-voltage part, whose configuration is shown in Fig. 1. The high-voltage part is composed of several half-bridge ac/dc converters connected in series through high-frequency transformers to cope with high input voltage, while the low-voltage part is composed of bidirectional half-bridge dc/dc converter and dc/ac inverter. Section II describes the grid-connected hybrid system below study. The block diagram representation grid connected hybrid system in Section III. Section IV describes the intelligent semiconductor

transformer. ANFIS control block diagram evaluated in Section V .Simulation was performed in section VI at last, Section VII establishes the conclusions resulting from this work.

II. GRID CONNECTED HYBRID SYSTEM FOR SMART GRID

The grid-connected hybrid system which is collected of power from WT and PV panels .Wind rectified ac voltage and PV voltage combined to dc-dc SEPIC converters in order to connect them to a central dc grid. In this system, the renewable sources are generating at any time there is wind or solar radiation.

A. Wind Turbine:

It presents a two-blade turbine coupled to a three-phase permanent magnet synchronous generator (PMSG).This WT is represented by a model with the following sub-systems: turbine and generation system. The generation system is composed of a three-phase PMSG, rectifier, and SEPIC converter, which are represented by models, are included [14]. Fig.2 shows the connects the WT to the hybrid system and dc grid, is controlled by a torque reference-based maximum power point tracking (MPPT) control in order to extract the maximum available power from the WT. This MPPT control maintains the operating point of the WT on its maximum power coefficient for any wind speeds in the below-rated wind speed region, modifying the duty cycle of the WT inverter, which produces a variation of its rotational speed.

B. PV Panels:

This model presents suitable precision [15], and the parameters are easy to find in the profitable datasheets, which makes it perfect for the simulation of PV devices with power converters. A SEPIC power converter controlled by an ANFIS controller adapts the PV output voltage to the dc grid voltage. The controller generates the duty cycle of the PV converter to move the PV voltage to the voltage that corresponds to the maximum power point (MPPT).

C. Single Ended Primary Inductor Converter (SEPIC):

This is a one type of dc-dc converter allow the electrical potential (voltage) at its output to be larger than, fewer than, or the same to that at its input and the output of the SEPIC is controlled by duty cycle of the control transistor. A SEPIC is basically a boost converter [1] followed by a buck-boost converter therefore it is like to a conventional buck-boost converter, but has compensation of having non-inverted output (the output has the same voltage polarity as the input), via a series capacitor to couple energy from the input to the output (and thus can respond more kindly to a short-circuit output), and being accomplished of true shutdown: when the switch is turned off, its output drops to 0 V.

D. Universal Bridge Rectifier:

Universal three-phase power rectifier that consists of up to six power switches associated in a bridge arrangement. The kind of power switch and converter pattern is selectable from the dialog box. The Universal Bridge block allows reproduction of converters by means of both naturally commutated (or line-commutated) power electronic devices (diodes or thyristors) and forced-commutated devices (GTO, IGBT, MOSFET).The Universal Bridge block is the

essential block for building two-level voltage-sourced converters (VSC).The device numbering is dissimilar if the power electronic [1] devices are naturally commutated or forced-commutated. For a obviously commutated three-phase rectifier (diode and thyristor), numbering follows the natural arrange of commutation.

E. Inverter:

H bridges are available as included circuits, or can be built from separate components. The word H Bridge is described from the typical graphical implementation of such a circuit. An H bridge is constructing with four switches. When the switches S1 and S4 are congested a positive voltage will be flow across the motor. By chance S1 and S4 switches and closing S2 and S3 switches, this voltage is inverted, following turn around operation of the motor.

III. BLOCK DIAGRAM REPRESENTATION OF GRID CONNECTED HYBRID SYSTEM WITH SMART GRID

In Fig.2 shows the block diagram of representation grid connected hybrid system with smart grid [2] used to home load application. Solar panel used to the home load and excess power send to the smart grid. BIST used for the purpose bidirectional power flow [3] direction. It consists of ac-dc rectifier dc-dc converter dc-ac inverter. Battery used for additional source for emergency purpose.

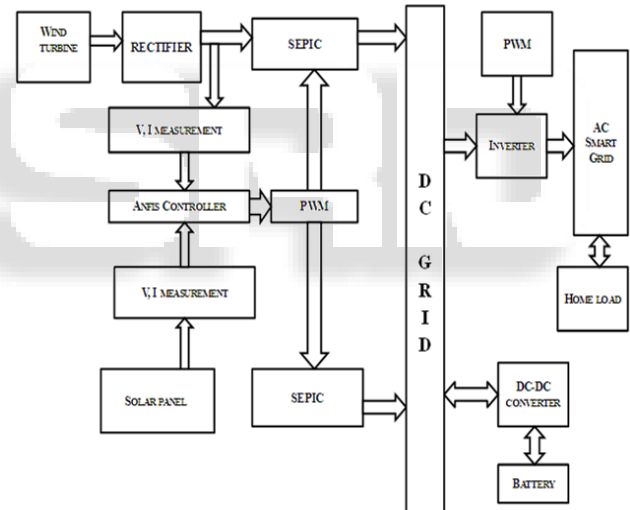


Fig. 2: block diagram representation of grid connected hybrid system with smart grid connected.

IV. INTELLIGENT SEMICONDUCTOR TRANSFORMER

A. High-Voltage Part:

The circuit of ac-dc converter, which converts single-phase ac voltage of into rectified dc.. The ac-dc converter has high-frequency transformers, which present high-frequency [10]-[12] resonance and input-output isolation. The input side works in high voltage, while the output side works in low voltage. Fig.3shows the high voltage part and low voltage part shows in Fig .6

The, the input side is considered with three half-bridge modules linked in series, in which two IGBT units are associated in series in the reverse direction. The output side is intended with three half-bridge modules linked in shunt. Total system operates in [11] bidirectional high-frequency resonance mode in a fixed frequency with 50%

duty ratio to decrease system size and switching loss. The switching pulses for each switch in a single-module of the bidirectional high-frequency ac/dc converter according to the polarity of the ac input voltage. The gating pulses for each switch are generated with same pattern power flow in a module.

B. Mode of Operation:

1) Mode 1:

The way of power flow is forward and the split of input voltage is positive. In the first stage, the primary current flows through the transistor in M1 and the diode in M2 when M1 turns ON. At this case, the secondary current flows through diode in M5. In the next point, the primary current allows through the transistor in M3 and the diode in M4 when M3 turns ON. At this case in point, the secondary current flows through the diode in M6.

2) Mode 2:

The way of power flow is forward and the division of input voltage is negative. In the first period, the primary current flows through the transistor in M2 and the diode in M1 when M2 turns ON. At this illustration, the secondary current flows through diode in M6. In the next point, the primary current flows through.

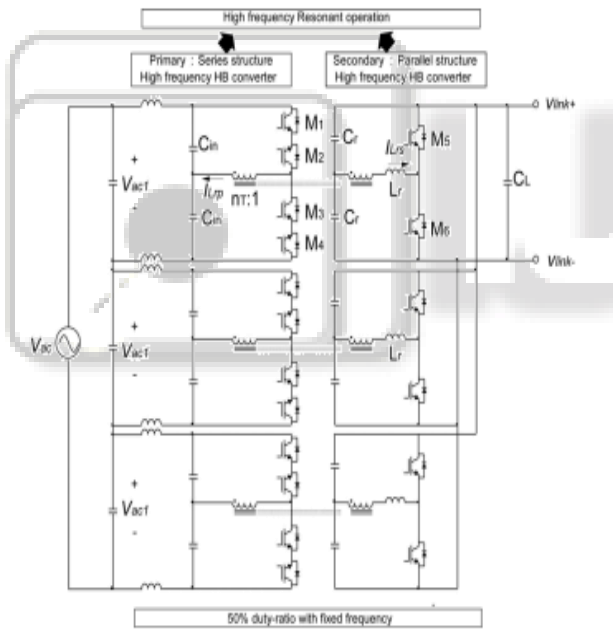


Fig. 3: Bidirectional intelligent semiconductor transformer.

3) Mode 3:

The direction of power flow is toward the back and the division of input voltage is positive. In the first step, the secondary current flows throughout transistor in M5 when M5 turn ON. At this illustration, the primary current flows through the diode in M1 and the transistor in M2.

4) Mode 4:

The way of power flow is toward the back and the split of input voltage is negative. In the first step, the secondary current flows all the way through transistor in M6 when M6 turn ON. At this illustration, the primary current flows throughout the transistor in M1 and the diode in M2. In the next step, the secondary current flow through the transistor

in M5 when M5 turns ON. At this example, the primary current flows all the way through the transistor in M3 and the diode in M4 shows in fig.5.

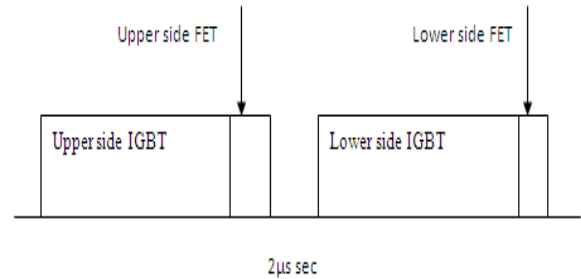


Fig. 4: Gating pulse method using IGBT and FET.

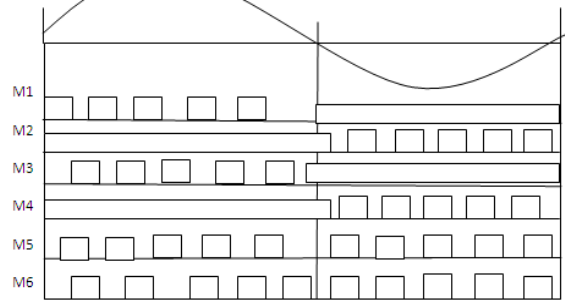


Fig. 5: High voltage resonant period signal of driving.

C. Low-Voltage Part:

The low-voltage part consists of the dc-dc converter and the dc-ac inverter joined in cascade as dc-dc converter changes the full-bridge ac rectified waveform into the constant dc voltage and the dc-ac inverter changes the constant dc voltage of into the single-phase ac voltage. The dc/dc converter and dc-ac inverter employ hybrid switch with IGBT and MOSFET coupled in parallel. The dc-dc converter and dc-ac inverter are composed of two half-bridges connected in cascade [9].

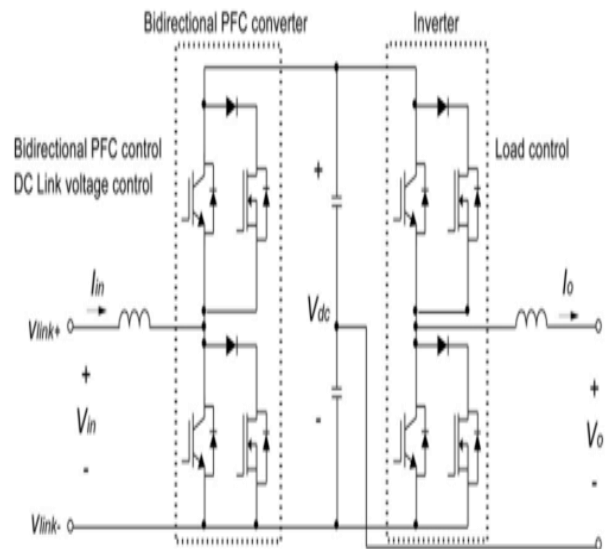


Fig. 6: Configuration of inverter and converter topology.

In regulate to get better this switching loss a MOSFET is coupled in parallel to apply a hybrid switch. Shows Fig.4 how to supply the gating signal to the hybrid switch. The MOSFET turns ON a only some microseconds further on while the IGBT switch turns OFF. Behind the MOSFET turns ON, the IGBT turns OFF directly and the

MOSFET turns OFF the immediate that the IGBT is initially to turn OFF shows in fig.7.

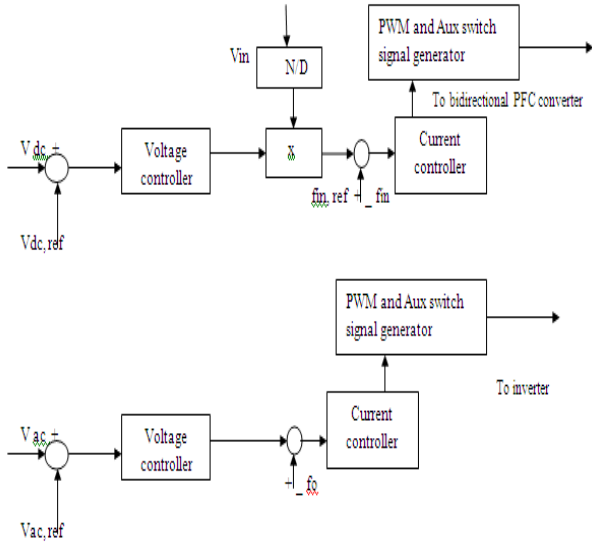


Fig. 7: Controller diagram of bidirectional dc-ac converter.

D. Zero-Voltage-Switching (ZVS):

In the operation given that the magnetizing inductance L_m cannot have infinity value in real transformer, operational modes are rather different from. As have explained in fig.8 and it is supportive to achieve soft-switching of switch [13]. All mode in have similar ZVS operation so that operational mode study is explained based on mode 1 of forward power flow with positive input voltage.

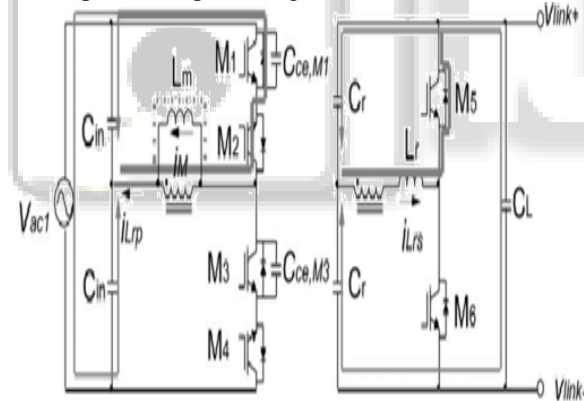


Fig. 8: ZVS operation mode.

E. Transformer Design:

The operational waveform of the LLC resonance converter [7]for the period of half of the line cycle. To examine the planned circuit, it is required to derive the resonant waveform expressions.

$$V_{ac1}[n] = V_{ac1,pk} \sin(\omega n T_{sr}) \quad (1)$$

$$V_{ink}[n] = (V_{ac1,pk} / \eta_T) \sin(\omega n T_{sr}) \quad (2)$$

The input voltage v_{ac1} and link voltage v_{link} for the period of n the switching period can be on paper as where ω means angular frequency of v_{ac1} and T_{sr} is resonant converter switching period. η_T means transformer turns-ratio

$$R_b = \frac{(V_{ac1,rms} / \eta_T)^2}{P_o} \quad (3)$$

The efficient resistor mode of secondary stage is only written as switch the output power of each resonant converter P_o . Referring to the resonant current waveforms

of both sides during n th switching period can be written as The primary resonant current I_{Lr} phase a small delay to the secondary resonant current I_{Lrs} since of the magnetizing current

$$i_{Lrp}[n] = \sqrt{2} I_{Lrp,rms}[n] \sin(2\pi f_{sr}(t - (n-1)T_{sr}) - \phi[n]) \quad (4)$$

$$i_{Lrs}[n] = \frac{\pi V_{ac1,pk} \sin(\omega n T_{sr})}{\eta_T R_b} \sin(2\pi f_{sr}(t - (n-1)T_{sr})) \quad (5)$$

Since v_{ac1} and v_{L} are understood to be constant during switching period, RMS current of I_{Lr} and the delayed angle of every switching period can be written as follows

$$i_{Lrp,rms}[n] = \frac{\pi V_{ac1,pk} \sin(\omega n T_{sr})}{\eta_T^2 R_b} \sqrt{\frac{\eta_T^4 R_b^2}{128 L_m^2 \omega^2 T_{sr}^2} + \frac{\pi^2}{2}} \quad (7)$$

where L_m is the magnetizing inductance referred to the primary side. The IGBT collector-emitter capacitance C_{ce} varies according to the magnitude of collector-emitter overvoltage.

V. SIMULATION RESULTS

The simulations were performed in classify to test the HRES controlled by the application ANFIS controllers by comparing it by means of the HRES controlled by the classical EMS. The initial one, Performed by the reproduction of the hybrid system operation during one year, was used to ensure the right presentation of the ANFIS-based supervisory control system in categorize to assure the power demanded by the grid

Smart distribution system. combine with converter, inverter and rectifier. Because load will not consumed this will act as a source. PWM controller send the gate pulse power will be return to grid. Fig.9 shows three ac voltage and current measured from wind turbine. Fig.10 shows the pv output voltage measured from pv array. They have light intensity value will be set some value then it will be varied with time. Fig.11 shows the wind and pv output voltage is variable one. It connected to the grid also it varied so it will be connected to the subsystem and fixed one after it will be connect to grid is a fixed one. Fig.12 shows the smart grid connected the load, using resistive will be connected 10 ohm.

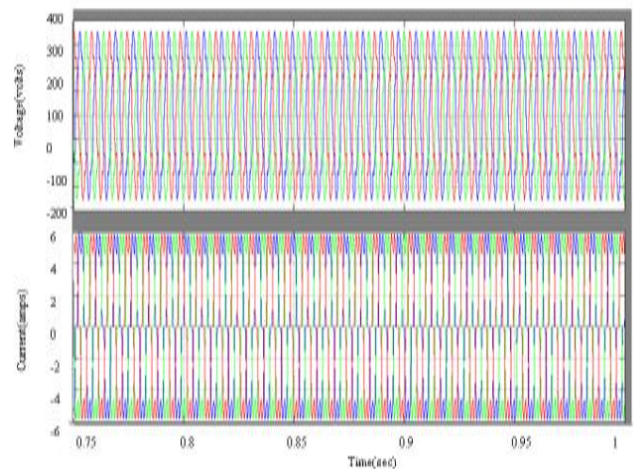


Fig. 9: Simulation diagram for three wind output voltage measured for wind turbine.

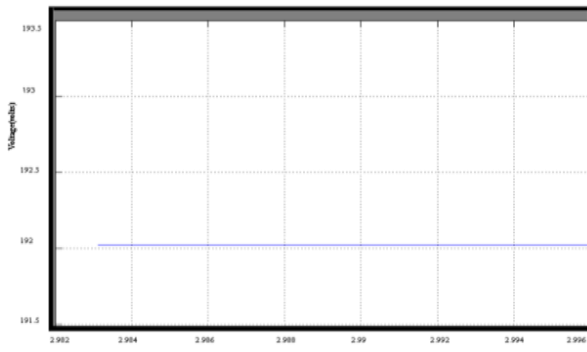


Fig. 10: Simulation diagram of voltage of the pv array.

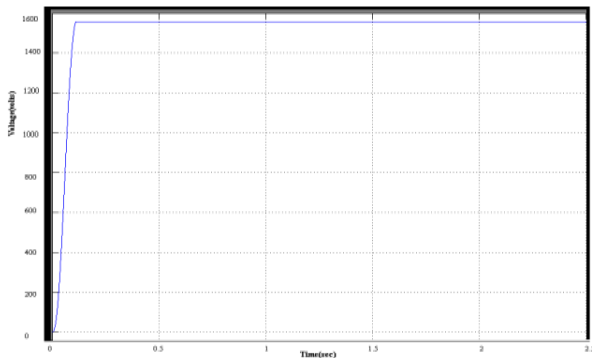


Fig. 11: simulation diagram of wind and solar output voltage connected to grid by using sepic converter.

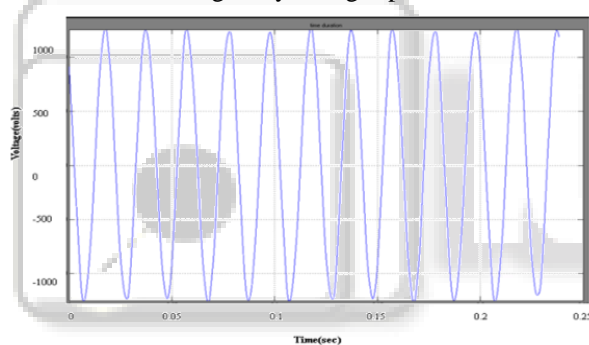


Fig. 12: Simulation diagram of smart grid distribution system connected to resistive load.

VI. CONCLUSION

In this paper has accessible and evaluated an ANFIS-based EMS of a grid-connected hybrid system, for smart grid which is composed of renewable energy sources (WT and PV panels). On the other hand, the coordination with the EMS, the single-phase inverter is controlled by an PWM-based controller in order to regulate the power. ANFIS-based EMS achieves better results, since it presents higher hybrid system efficiencies, and it is capable of injecting more energy into grid than the classical EMS. The results of both simulations and demonstrated that the proposed EMS allows a better control than the classical EMS and reliable operation in grid-connected application. The short scale operation shows the right dynamic response of the hybrid system and inverter against sudden power variations and its effect on the dc bus voltage and three-phase waveform of the inverter output voltage and current. In this case, the inverter controlled with ANFIS presents lower error indexes and THD than those obtained with the controllers. The operational feasibility of the transformer was verified by

computer simulation with PSCAD/EMTDC software based on the simulation results.

REFERENCES

- [1] M. Jamil, B. Hussain, M. Abu-Sara, R. J. Boltryk, and S. M. Sharkh, "Microgrids power electronic converters: State of the art and future changes," in Proc. 44th Int. Universities Power Eng. Conf., 2009, pp. 1–5.
- [2] P. Siano, C. Cecati, H. Yu, and J. Kolbusz, "Real time operation of smart grids via FCN networks and optimal power flow," IEEE Trans. Ind. Inf., vol. 8, no. 4, pp. 944–952, Nov. 2012.
- [3] S. Jiang, W. Wang, H. Jin and Xu, "Power management strategy for microgrid with energy storage system," in Proc. 37th Annu. Conf. IEEE Ind. Electron. Soc., pp. 1524–1529.
- [4] L. Valverde, F. Rosa, and C. Bordons, "Design, planning and management of a hydrogen-based microgrid," IEEE Trans. Ind. Inf., vol. 9, no. 3, pp. 1398–1404, Aug. 2013.
- [5] M. P. Kazmierkowski, M. Jasinski, and G. Wrona, "DSP-based control of grid-connected power converters operating under grid distortions," IEEE Trans. Ind. Inf., vol. 7, no. 2, pp. 204–211, May 2011.
- [6] M. N. Marwali, J. W. Jung, and A. Keyhani, "Control of distributed generation systems – Part II: Load sharing control," IEEE Trans. Power Electronics., vol. 19, no. 6, pp. 1551–1561, Nov. 2004.
- [7] M. Kang, P. Enjeti, and I. Pitel, "Analysis and design of electronic transformers for electric power distribution system," IEEE Trans. Power Electron., vol. 14, no. 6, pp. 1133–1141, Nov. 1999.
- [8] S. N. Bhaskara and B. H. Chowdhury, "Microgrids – A review of modeling, control, protection, simulation and future potential," in Proc. IEEE Power and Energy Soc. Gen. Meeting, 2012, pp. 1–7.
- [9] M. Arindam, S. Ashok, G. Mahesh, B. Simon, and D. Shoubhik, "Intelligent universal transformer design and applications," in Proc. 20th Int. Conf. Exhib. Elect. Distrib., 2009, pp. 1–7.
- [10] "Feasibility assessment for intelligent universal transformer," EPRI, Palo Alto, CA, USA, EPRI Rep. TR-1001698, Dec. 2002.
- [11] E. C. Aeloiza, P. N. Enjeti, L. A. Moran, and I. Pitel, "Next generation distribution transformer: To address power quality for critical loads," in Proc. IEEE Annu. Power Electron. Spec. Conf., 2003, pp. 1266–1271.
- [12] Z. Tiefu, Z. Jie, S. Bhattachaya, M. E. Baran, and A. Q. Huang, "An average model of solid state transformer for dynamic system simulation," in Proc. IEEE Power Energy Soc., 2009, pp. 1–8.
- [13] S. Dasgupta, S. N. Mohan, S. K. Sahoo, and S. K. Panda, "A plug and play operational approach for implementation of an autonomous micro-grid

- system,"IEEE Trans. Ind. Inf., vol. 8, no. 3, pp. 615–629, Aug. 2012
- [14] J. I. Rosell and M. Ibáñez, "Modelling power output in photovoltaic modules for outdoor operating conditions," *Energ. Convers. Manag.*, vol. 47, no. 15–16, pp. 2424–2430, Sep. 2006.
- [15] M. G. Villalva, J. R. Gazoli, and E. R. Filho, "Comprehensive approach to modeling and simulation of photovoltaic arrays," *IEEE Trans. Ind. Electron.*, vol. 24, no. 5, pp. 1198–1208, May 2009.

